Carbothermic reduction of a willemite concentrate for use in the Waelz process

by V.S. Coimbra[1], G.M. de Lima[2], V.A. Leão[3], R.F.M. de Souza[4], and V.A.A. Oliveira[1]

Affiliation:
[1]Pyrometallurgy and Thermal Analysis Laboratory, Department of Metallurgical and Materials Engineering, Universidade Federal de Ouro Preto, Ouro Preto, Minas Gerais, Brazil.
[2]Coordination Chemistry Laboratory, Department of Chemistry, Universidade Federal de Minas Gerais, Belo Horizonte, Minas Gerais, Brazil.
[3]Bio&Hidrometalurgia Laboratory, Department of Metallurgical and Materials Engineering, Universidade Federal de Ouro Preto, Ouro Preto, Minas Gerais, Brazil.
[4]Pyrometallurgy Research Group, Department of Chemical and Materials Engineering, Pontifícia Universidade Católica do Rio de Janeiro, Rio de Janeiro, Rio de Janeiro, Brazil.

Correspondence to:
V.A.A. Oliveira

Email:
victor@ufop.edu.br

Dates:
Received: 12 Dec. 2022
Accepted: 24 Aug. 2023
Published: November 2023

How to cite:
Coimbra, V.S., de Lima, G.M., Leão, V.A., de Souza, R.F.M., and Oliveira, V.A.A. 2023
Carbothermic reduction of a willemite concentrate for use in the Waelz process. Journal of the Southern African Institute of Mining and Metallurgy, vol. 123, no. 11. pp. 513–520

DOI ID:
http://dx.doi.org/10.17159/2411-9717/2516/2023

ORCID:
V.S. Coimbra
http://orcid.org/0000-0003-1891-548X
G.M. de Lima
http://orcid.org/0000-0002-3816-0320
V.A. Leão
http://orcid.org/0000-0001-9495-6529
R.F.M. de Souza
http://orcid.org/0000-0002-3468-686X
V.A.A. Oliveira
http://orcid.org/0000-0003-2099-9459

Synopsis

A willemite concentrate consisting mainly of willemite (55.3%) and dolomite (15.6%) was reduced in a tube furnace with charcoal as reductant. The effects of temperature and varying reductant additions on zinc extraction were studied. A zinc recovery of 86% was achieved with 20% reductant in the charge at 1100°C. During reduction, the calcium oxide generated through calcination of the dolomite promoted decomposition of the willemite, thus lowering the temperature at which reduction took place. The presence of CaO improved the zinc recovery at all temperatures studied. The best zinc recovery (93%) was obtained in the presence of 5% CaO, 20% charcoal reductant, and at a temperature of 1100°C. The results show that the willemite concentrate studied has great potential to be used as a raw material for the Waelz process.

Keywords

willemite, carbothermic reduction, zinc smelting, Waelz process, non-sulphide zinc ore, calcium oxide.

Introduction

Sphalerite (ZnS) is the main source of zinc, which is obtained through a roast-leach-electrowinning (RLE) process (Souza *et al.*, 2007a; Sinclair, 2005; Safari *et al.*, 2009). In general, in this process, the sphalerite concentrate is roasted in a fluidized bed furnace to obtain zinc oxide. The main solid products of roasting (ZnO and $ZnFe_2O_4$) are leached in tanks using sulphuric acid, and after purification, zinc-rich liquor is sent to the aqueous electrolysis stage to obtain zinc cathode (Special High-Grade Zinc – 99.995% Zn) (Sinclair, 2005; Oliveira *et al.*, 2019).

Other zinc minerals of economic importance are smithsonite ($ZnCO_3$) and willemite (Zn_2SiO_4) (Souza *et al.*, 2007b; Li *et al.*, 2013). These minerals are constituents of secondary zinc deposits, called calamine deposits (Zhang *et al.*, 2018; Boni and Mondillo, 2015). These minerals occur in non-sulphide zinc ores (Souza *et al.*, 2007b). These ores are not processed by RLE for various reasons. Dehydration and/or calcination is an endothermic reaction that will lead to higher energy consumption, in contrast to the exothermic roasting reaction (Zhang *et al.*, 2019; Zhao *et al.*, 2017; Xiong *et al.*, 2012; Liu *et al.*, 2012). The presence of acid-consuming minerals in the gangue (dolomite and calcite) will result in the consumption of large amounts of sulphuric acid during leaching (Santos *et al.*, 2010). Acid leaching solubilizes a great deal of silica, which forms silica gel (Souza *et al.*, 2007a; Xiong *et al.*, 2012; Safari *et al.*, 2009; Liu *et al.*, 2012; Yin *et al.*, 2010). Furthermore, non-sulphide zinc minerals pose greater challenges during the concentration stages (Zhao *et al.*, 2017), hence, the zinc contents of the concentrates are lower than those obtained from sulphide ores.

A possible alternative route for the extraction of zinc from these ores involves alkaline leaching (Santos *et al.*, 2010). This would avoid the excessive consumption of acid reagents by the gangue minerals and the high energy demand associated with endothermic reactions (Zhang *et al.*, 2014; Liu *et al.*, 2012). Several alkaline reagents, such as NH_4OH/NH_4Cl and $NaOH/NH_4Cl$, have been used in the leaching of these ores (Santos *et al.*, 2010; Zhang *et al.*, 2019; Li *et al.*, 2013; Zhao *et al.*, 2017; Liu *et al.*, 2012; Yin *et al.*, 2010). However, these reagents are considerably more expensive than sulphuric acid. In addition, the authors are not aware of any process that uses alkaline leaching of non-sulphide zinc ores on an industrial scale.

A classic metallurgical process used for treating various zinc-bearing residues is the so-called Waelz process. This process has been extensively used and is a safe and reliable technology applied for the recovery of metals such as Pb, Cd, Ge, and particularly Zn, from electric arc furnace dust (EAFD) and other steel industrial residues (Chen, 2001; Mager *et al.*, 2000; Antuñano, Arias, and Cambra, 2019, 2013; James and Bound,). EAFD is a waste, formed during steel production, which contains considerable amounts of zinc (Xiong *et al.*, 2017). For zinc recovery from zinc-bearing residues, the Zn^{2+} cation is usually reduced in a rotary furnace (the Waelz furnace) at 1200°C, using a carbonaceous reducing agent. The reduction of zinc

oxide by carbon occurs at a temperature higher than the boiling point of the metal (907°C), and consequently the zinc vaporizes (Xiong *et al.*, 2017; Antuñano, Arias, and Cambra, 2019):.

$$ZnO(s) + C(s) \rightarrow Zn(g) + CO(g) \quad \Delta G^0_{T>1229K} < 0 \qquad [1]$$

Due to the oxidizing atmosphere in the Waelz furnace the Zn metal that evaporates from the reduction reaction zone is oxidized in contact with this gaseous phase (Equations [2] and [3]), forming a very fine powder (ZnO) which is collected in the bag filter (Antuñano, Arias, and Cambra, 2019).

$$2Zn(g) + O_2(g) \rightarrow 2ZnO(s) \quad \Delta G^0 = 212.7T - 708{,}610 \left(\frac{J}{mol\ O_2}\right) \qquad [2]$$

$$Zn(g) + CO_2(g) \rightarrow ZnO(s) + CO(g) \quad \Delta G^0 = 118.5T - 189{,}460 \left(\frac{J}{mol\ O_2}\right) \qquad [3]$$

This powder is called Waelz oxide and, after purification (dehalogenation), it can be added to the acid leaching step of the RLE process. In this way, it is possible to recover zinc from secondary sources in an integrated way. A comprehensive review of the pyrometallurgical recovery of zinc from EAFD was presented by Wang *et al.* (2021). The fundamentals and operational parameters of the Waelz process , which is applied to the recovery of zinc and other volatile metals from secondary zinc resources, were described by Harris (1936).

As well as being an important metallurgical approach for the treatment of non-sulphide zinc ores, the Waelz process is often used for the recovery of zinc from secondary sources. These sources usually have a lower zinc content (*e.g.* 22–28% Zn for EAFD) compared to oxidized ore concentrates (Xiong *et al.*, 2017; Antuñano, Arias, and Cambra, 2019). It is noteworthy that the utilization of non-sulphide concentrates as feed to the Waelz process has received less attention than zinc-bearing residues.

Many zinc-bearing residues are very heterogeneous in terms of their chemical composition and moisture content. For instance, many the raw materials used in the Waelz process often consist of a blend of different zinc-containing materials (Krupka *et al.*, 2000; Mager *et al.*, 2000; Harris, 1936). The study of the mineralogical changes under the typical operating conditions of the Waelz process can therefore contribute to a better understanding of the process in general.

We studied the influence of temperature, the presence of CaO, and the amount of charcoal on the extraction of zinc from a willemite concentrate. Mineral transformations associated with the carbothermic reduction of this mineral and the gangue constituents were also investigated to determine chemical reactions that may occur if a willemite concentrate alone is fed to a Waelz furnace.

Materials and methods

The willemite concentrate (CW) was supplied by Nexa Resources from a mine in the northwest region of the Brazilian state of Minas Gerais. The as-received sample had a moisture content of approximately 15% and particle size 100% less than 75 µm. All experiments were carried out had been samples that dried in an oven for 48 hours at 105°C.

Chemical analysis

Approximately 0.150 g of the sample was homogenized with 4 g of a mixture of 1 part sodium tetraborate (Synth, 99.5%) to 3 parts sodium carbonate (F. Maia, 99.5%) and fused in a platinum crucible at 950°C for 40 minutes in a muffle oven. After fusion, all material was dissolved in an acid solution (HCl approx. 18% v/v). The solution was analysed by inductively coupled plasma optical emission spectrometry (ICP-OES, Varian model 725).

X-ray diffractometry

X-ray diffractograms were obtained using a Shimadzu model XRD-6100 diffractometer equipped with a copper source operating at 45 kV and 40 mA and with a 1°/min scanning speed. The main phases in the samples were identified by comparison with standard diffractograms (ICSD patterns) using DIFFRAC.EVA. TOPAS 5.0 software was used to quantify the mineral phases present in the sample using the Rietveld method.

Thermogravimetric analysis

Thermogravimetric curves were obtained using a heating rate of 10°C/min in an inert atmospere of N_2 (White Martins, 99.9990%) at a flow rate of 50 ml/min. We used a Shimadzu model DTG 60 thermogravimetric analyser.

Scanning electron microscopy (SEM) and X-ray energy dispersive spectroscopy (EDS)

The sample was embedded in polyester resin and, after drying, the surface was polished using silicon carbide paper of different grain sizes (150 to 1500 grit). After sanding, the surface was polished with alumina paste (1 µm). The surface of the sample was metallized with gold using a sputter coater (Quorum model Q150R ES). The SEM images were generated using a Tescan model Vega 3 LMH and EDS mapping was performed using an Oxford INCA x-act 51-ADD0007 instrument.

Reduction experiments

Charcoal (CV) ground to 100% less than 300 µm was used as reductant. Volatiles were removed by heating the ground charcoal sample in a closed crucible for 1 hour at 1000°C in a muffle furnace. Mixtures with different CW/(CW + CV) ratios were prepared and homogenized for the experiments, to evaluate the influence of CV on the reduction. The influence of calcium oxide on the reduction was assessed by adding different amounts of CaO to the CW/(CW + CV) mixture. A crucible containing approximately 5 g of the reaction mixture was placed in a Jung tubular furnace with an automatic temperature controller, and a continuous flow (2 L/min) of N_2 (99.9990%) was maintained inside the furnace throughout the experiment. After reduction, the crucible was heated in a muffle furnace at 800°C for 2 hours to remove residual carbon. Zinc extraction (Zn%) from CW was calculated according to Equation [4]:

$$Zn\% = \frac{m_0^{CW} - m_f^{CW}}{m_0^{CW}\ x\ i_{ZnO}} \qquad [4]$$

where m_f^{cw} is the final mass of CW after reduction and removal of excess CV, m_0^{cw} is the initial mass of CW, and ZnO is the zinc oxide content in the CW sample. For the experiments where the influence of CaO was investigated, the mass of this reagent added at the beginning of the experiment was subtracted from the final mass after the removal of excess CV. All experiments were done in triplicate. Duplicates of the blank experiments were performed for all experimental conditions studied and the mass loss found for these experiments was added to the mass of m_f^{cw}.

Thermodynamic data

HSC Chemistry V 4.1 software was used to construct the equilibrium diagrams.

Table I

Chemical analysis of the willemite concentrate (CW) (%)

Zn	Ca	Mg	Fe	Al	Pb	Cd
32.5	4.6	2.8	4.9	0.4	0.3	0.025

Results and discussion

Characterization of willemite concentrate

The chemical analysis of the concentrate is shown in Table I. The Zn content, 32.5% is considerably higher than the values reported by different authors for EAFD (20-28%) and other zinc-bearing materials (Mattich *et al*., 1998; Xiong *et al*., 2017). This is another attractive reason to use this material as feed to a Waelz furnace.

Figure 1 shows both the X-ray diffractograms for the sample, one obtained by experiment and the other provided by the Rietveld method, revealing good concordance of results. Willemite (53.3%) is the main constituent, followed by dolomite (15.6%) (Table II). Table II also shows that three Zn-bearing minerals were identified: smithsonite (2.3%), hydrozincite (2.7%), and willemite (53.3%). Thus, 91.7% of the Zn present in the sample is in willemite, 3.5% in smithsonite, and 4.7% in hemimorphite. The minerals identified in the concentrate are typical minerals of this type of ore (Dill, 2010).

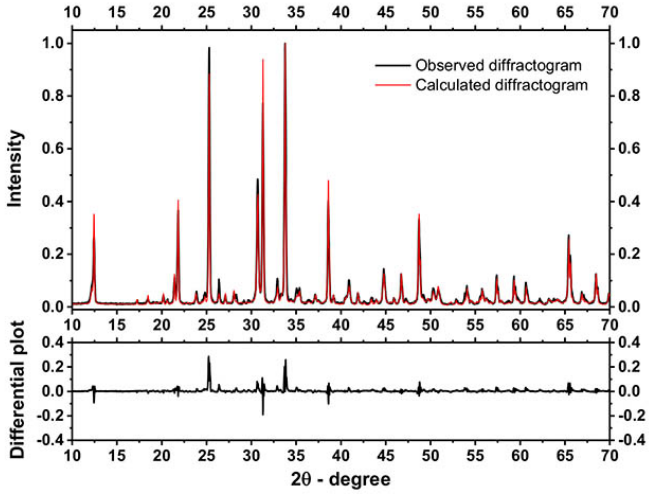

Figure 1—X-ray diffractogram for the CW sample

Table II

Mineralogical composition of the sample

Mineral	Formula	Content (%)
Willemite	Zn_2SiO_4	53.3
Dolomite	$CaMg(CO_3)_2$	16.4
Chlorite	$H_4Mg_3Si_2O_9$	8.3
Nacrite	$Al_2(Si_2O_5)(OH)_4$	6.5
Quartz	SiO_2	4.7
Hydrozincite	$Zn_5(CO_3)_2(OH)_6$	2.7
Smithsonite	$ZnCO_3$	2.3
Kaolinite	$Al_4(Si_4O_{10})(OH)_8$	2.0
Monticelite	$CaMgSiO_4$	2.8
Others	–	1.0

The difference between the zinc values found by ICP-OES (32.5%) and by the Rietveld method (34.1%) is less than 5%.

Figure 2 shows the TGA and DTG curves for the decomposition of the CW sample in an inert atmosphere. The curves show two mass loss events in the temperature range between 478°C and 790°C. These events are identified as (i) and (ii) on the DTG curve. According to the mineralogical analysis, event (i) can be attributed to the thermal decomposition of smithsonite and hydrozincite according to Equations [5] and [6]:

$$ZnCO_3 \rightarrow ZnO + CO_2 \quad \Delta G^0 = -125.8T + 30{,}114\ (\tfrac{J}{mol}) \qquad [5]$$

$$Zn_5(CO_3)_2(OH)_6 \rightarrow 5ZnO + 2CO_2 + 3H_2O \quad \Delta G^0 = -457.9T + 79{,}726\ (\tfrac{J}{mol}) \qquad [6]$$

The mass loss shown in the TGA curve associated with the event (i) is 1.55%. According to the results obtained using the Rietveld method, for a sample containing 2.3% smithsonite and 2.7% hydrozincite (Table II), the expected mass losses will be 0.807% and 0.698%, respectively. Therefore, the total mass loss associated with the decomposition of smithsonite and hydrozincite will be approximately 1.5%, which is very close to that shown in the TGA curve. The temperature values found for the thermal decomposition of these minerals agree with the results of other authors (Wahab *et al*., 2008; Wang *et al*., 2021)). The event (ii) in the TGA curve is attributed to the thermal decomposition of dolomite according to Equation [7]:

$$CaMg(CO_3)_2 \rightarrow CaO + MgO + 2CO_2 \quad \Delta G^0 = -321.7T + 292{,}100\ (\tfrac{J}{mol}) \qquad [7]$$

The free energy values show that the temperature of thermal decomposition (calcination) of dolomite is 908K (635°C), considering the standard state (pCO_2 = 1 atm.) and the activity of solid species equal to the unit. It is important to highlight that the experimental condition is not the standard state, but the calculated thermodynamic temperature of calcination is within the temperature range obtained experimentally. In addition, the values found are in accordance with the results of some research groups (Herce, Stendardo, and Cristóbal, 2015; Ptáček, Šoukal, and Opravil, 2021). The evidence for the decomposition of dolomite, hemimorphite, and smithsonite in the proposed temperature range

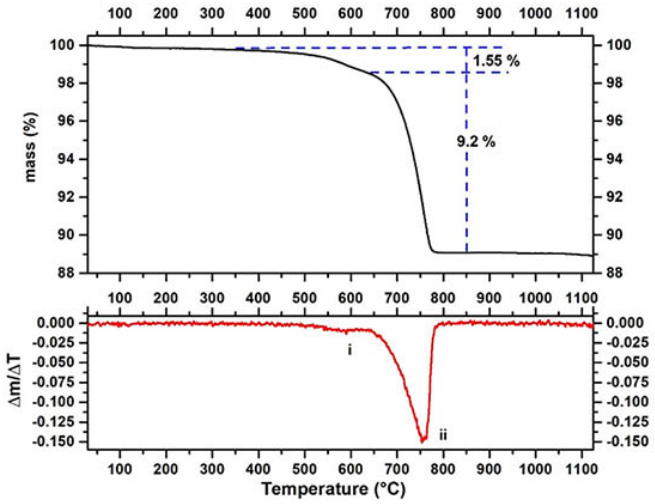

Figure 2—TGA curves and DTG of CW sample decomposition in an inert atmosphere (N_2 50 ml/min) at a heating rate of 10°C/min

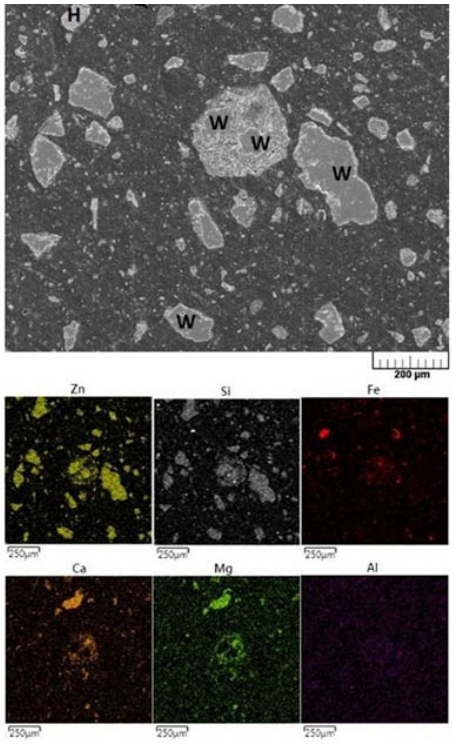

Figure 3—SEM-EDS images for willemite concentrate sample. (W) willemite; (D) dolomite; (Q) quartz; (H) magnetite

could be confirmed by the disappearance of the diffraction peaks characteristic of these minerals when the sample was calcined in a muffle furnace at a temperature of 810°C (*c.f.* Figure 8). Finally, the results show that for a mass loss of 9.2%, the sample contains about 19.2% dolomite (*c.f.* Equation [7]). The dolomite content calculated through the TGA curve is very close to the value obtained using the Rietveld method for mineralogical quantification.

Figure 3 shows a SEM image and EDS mapping for the CW sample. The main constituent minerals were identified through the association of phases identified in the X-ray diffractogram, with the elemental associations revealed by EDS mapping.

Carbothermic reduction of the willemite concentrate

Thermogravimetry

Figure 4 shows the thermogravimetric curve for the reduction of willemite concentrate. Two thermal events, A and B, can be identified. These events are due to (A) dolomite calcination, smithsonite calcination, and dehydration, and calcination of hemimorphite (Equations [5], [6], and [7]), and (B) the reduction of willemite. Equations [8] and [9] show two possible reactions of willemite reduction and Figure 5 shows the Ellingham diagram for these reactions.

$$Zn_2SiO_4 + C \rightarrow 2Zn_{(g)} + CO_{2(g)} + SiO_2 \quad \Delta G^0 = -391.4T + 559\,700\ (\tfrac{J}{mol}) \quad [8]$$

$$Zn_2SiO_4 + 2C \rightarrow 2Zn_{(g)} + 2CO_{(g)} + SiO_2 \quad \Delta G^0 = -562.8T + 726\,410\ (\tfrac{J}{mol}) \quad [9]$$

The results show that above 1291K (1018°C) the reduction of willemite, generating CO(g) as a reaction product becomes spontaneous. Therefore, this is one of the possible reactions

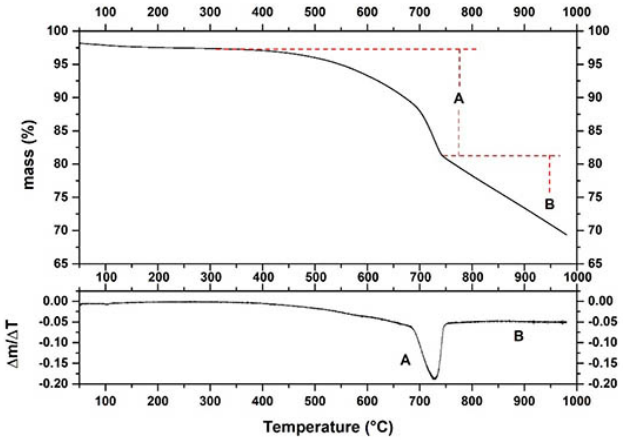

Figure 4—TGA and DTG curves for the reduction of willemite concentrate with charcoal (40% w/w) in an inert atmosphere at s heating rate of 10°C/min

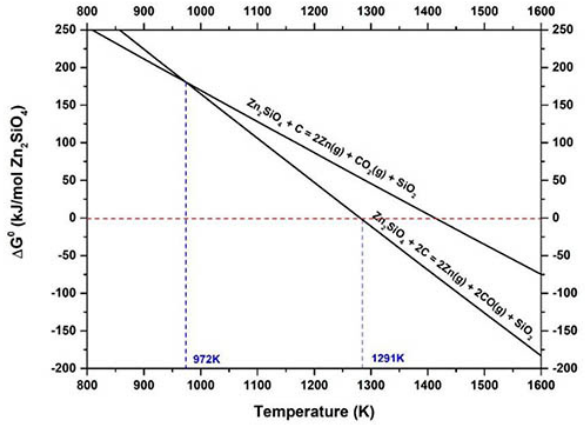

Figure 5—Ellingham diagram for the carbothermic reduction of willemite

responsible for the second event on the TGA curve. It is also worth mentioning that, as shown in the diagram, this reaction will be thermodynamically more favourable than the reaction where CO_2 is formed, at any temperature higher than 972K (699°C).

Gaseous carbon monoxide, formed *in situ*, is a possible reducing agent playing a role in the extraction of Zn from willemite. Equations [10], [11], and [12] represent the possible reactions.

$$Zn_2SiO_4 + CO(g) \rightarrow CO_2(g) + Zn(g) + SiO_2 \quad \Delta G^0 = -233.9T + 409\,900\ (\tfrac{J}{mol}) \quad [10]$$

$$SiO_2 + CO(g) \rightarrow CO_2(g) + Si \quad \Delta G^0 = 0.9T + 338\,140\ \left(\tfrac{J}{mol}\right) \quad (1000K < T < 1500K) \quad [11]$$

$$CO_2(g) + C \rightarrow 2CO(g) \quad \Delta G^0 = -173.4T + 169\,320\ (\tfrac{J}{mol}) \quad [12]$$

Figure 6 shows the variation of $\log(pCO/pCO_2)$ as a function of temperature for willemite reduction. The diagram shows that the solid products are Zn and SiO_2. These results indicate that SiO_2 does not reduce in such conditions.

In the TGA curve, the event attributed to the reduction of willemite starts at a temperature lower than that indicated by thermodynamic data (approx. 950°C) and, therefore, the observed mass loss for temperatures lower than 1018°C cannot be attributed to the reactions represented by Equations [9] and [10]. Thus, the

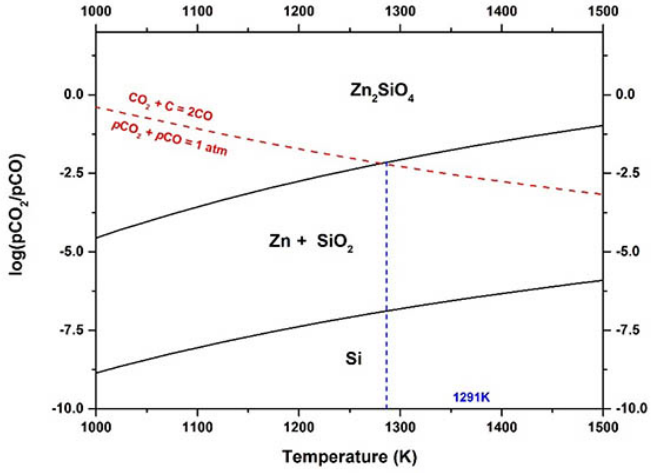

Figure 6—log(pCO_2/pCO) as a function of temperature for the reduction of willemite

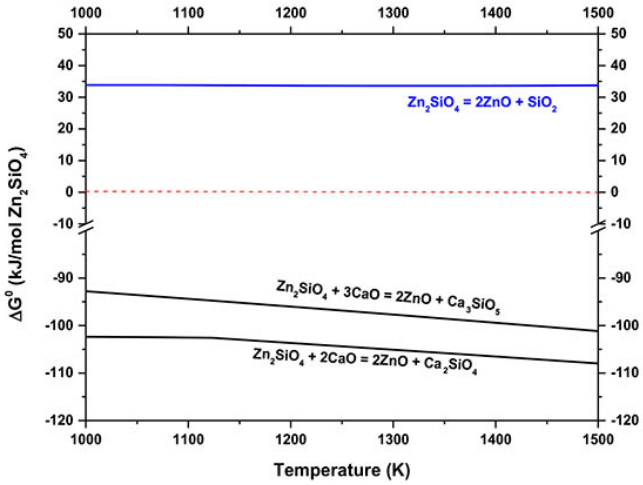

Figure 7—Ellingham diagram for willemite decomposition reactions

results suggest that the calcium oxide generated by the calcination of dolomite promotes the decomposition of willemite, generating different calcium silicates and zinc oxide. Equations [13] and [14] show some of the possible chemical reactions involved in willemite decomposition, and Figure 7 shows that these reactions are thermodynamically favourable throughout the studied range of temperature. Finally, the diagram also shows that the decomposition of willemite in the absence of these oxides is not thermodynamically favourable (blue line).

$$Zn_2SiO_4 + 2CaO \rightarrow 2ZnO + Ca_2SiO_4 \quad \Delta G^0 = -14.T4 - 86\,416\ (\tfrac{kJ}{mol}) \quad [13]$$

$$Zn_2SiO_4 + CaO \rightarrow 2ZnO + Ca_3SiO_5 \quad \Delta G^0 = -15.5\,T - 77\,622\ \left(\frac{kJ}{mol}\right) \quad [14]$$

Figure 8 shows the X-ray diffractograms for the samples decomposed at 800°C and 1100°C. Diffraction peaks characteristic of zinc oxide and different calcium silicates can be identified. It is noteworthy that although the formation of different magnesium silicates is thermodynamically favourable in this temperature range, only diffraction peaks characteristic of a mixed calcium and magnesium silicate ($CaMgSiO_4$, montcellite) could be identified. The Rietveld method was not applied to quantify the generated phases because the reaction between these basic oxides (CaO and MgO) and silica produces too many amorphous phases.

The results show that the calcium oxide generated during the thermal decomposition of dolomite reacts with willemite forming ZnO and different calcium silicates. Note the presence of ZnO in the diffractograms in Figure 8. The zinc oxide formed is reduced by carbon and/or carbon monoxide according to Equations [15], [16], and [17]:

$$2ZnO + C \rightarrow CO_2(g) + 2Zn(g) \quad \Delta G^0 = -410.3T + 548\,240\ \left(\frac{J}{mol\ C}\right) \quad [15]$$

$$ZnO + C \rightarrow CO(g) + Zn(g) \quad \Delta G^0 = -291.8T + 358\,780\ \left(\frac{J}{mol\ C}\right) \quad [16]$$

$$CaO + CO_2 \rightarrow CaCO_3 \quad \Delta G^0 = 147.6T - 172\,070\ (\tfrac{J}{mol\ CO_2}) \quad [17]$$

The standard free energy values for the reactions show that ZnO can be reduced by carbon at a temperature lower than willemite – 1229.5K (956°C), which justifies the low temperatures at the

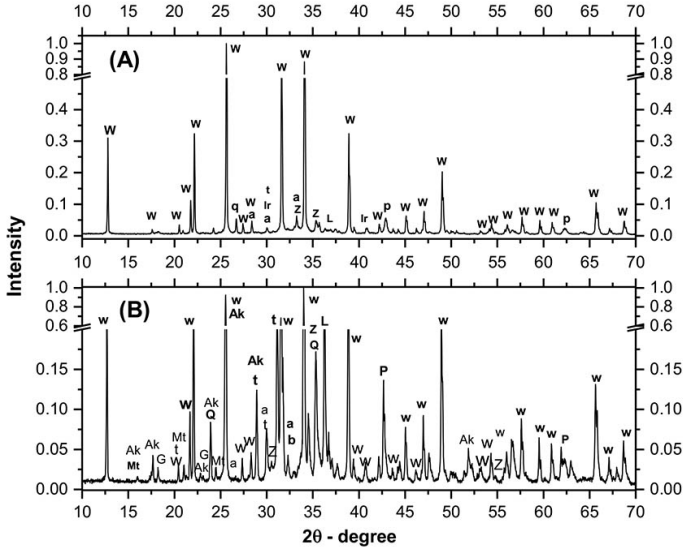

Figure 8—X-ray diffractogram for the WC sample calcined at (A) 800°C and (B) 1100°C. (w) willemite – Zn_2SiO_4; (q) quartz – SiO_2; (a) alite; (t) walstromite - $CaSiO_3$; (lr) larnite - Ca_2SiO_4; (L) lime - CaO; (z) zincite – ZnO; (p) periclase - MgO; (Mt) montcelite - $CaMgSiO_4$; (Ak) akermanite; (G) gehlenite; (b) Ca_3SiO_5

beginning of the CW sample reduction. Figure 9 shows the log diagram of (pCO_2/pCO) as a function of temperature for the zinc oxide reduction reaction, where it can be seen that this oxide will be reduced by a less reducing pCO_2/pCO mixture than that required to reduce willemite.

Since the presence of calcium oxide in the sample decreased the minimum temperature required for reduction, thermogravimetric carbothermic reduction assays in the presence of CaO (20% w/w) were performed to verify the influence of CaO on the process. Figure 10 shows the thermogravimetric curve of CW reduction in the presence of CaO, where one can observe the same events A and B, present in the TG curve for willemite concentrate reduction (Figure 4). The results show that in the presence of CaO, the mass loss was higher, suggesting the reduction of a greater amount of zinc oxide.

Finally, in addition to events A and B, a new thermal event (event Y) could be observed in the TG and DTG curves when calcium oxide is added to the system. The authors believe that the mass loss observed in event Y can be attributed to the beginning of dolomite decomposition and to the reduction of metal oxides (Pb and Cd) that are always present in zinc ores. These reactions release CO_2, which reacts with the calcium oxide (carbonation) forming calcium carbonate (Equation [18]), it is worth noting that calcium oxide carbonation is thermodynamically favourable at temperatures lower than 950°C.

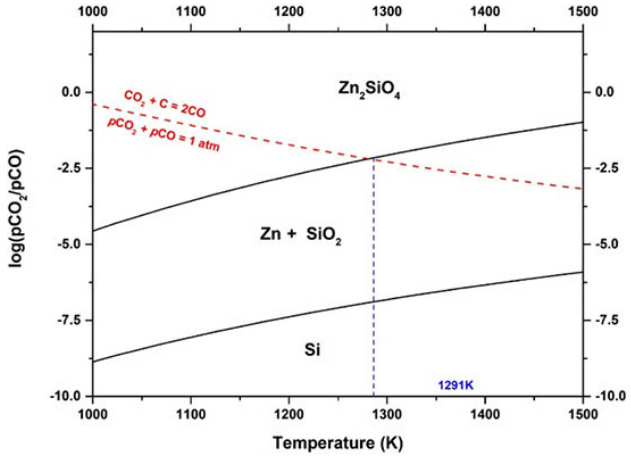

Figure 9—Diagram of log(pCO_2/pCO) as a function of temperature for the Zn-O-C system

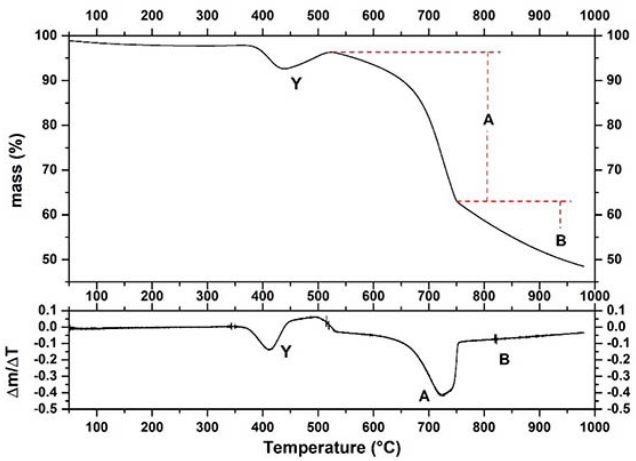

Figure 10—TGA and DTG curves for the reduction of willemite concentrate with charcoal (40% w/w) in the presence of calcium oxide (20% w/w) in an inert atmosphere (N_2 50 ml/min) at a heating rate of 10°C/min

$$ZnO + CO(g) \rightarrow CO_2(g) + Zn(g) \quad \Delta G^0 = -118.5T + 189\,460 \left(\frac{J}{mol\ CO}\right) \quad [18]$$

Experiments in a horizontal tube furnace

Before being reduced in a horizontal tube furnace, CW samples were calcined at a temperature of 810°C. This eliminated the thermal event associated with dolomite calcination and ensured that, in the zinc extraction calculations, the mass loss values obtained could be attributed only to the reduction of zincite and willemite (Equations [1] and [9]).

After verifying the minimum temperature for the reduction of the CW sample from the TGA curves, reduction experiments were carried out in a horizontal tube furnace at a temperature of 1100°C, varying the amount of CV added to the system. Figure 11 shows the zinc extraction values obtained in these experiments. As can be seen, the extraction values were constant when the amount of CV added was greater than 20%; it is important to stress that the stoichiometric amount required for the reduction would be approximately 11% (Equation [9]). The results also show that using 20% C at 1100°C it was possible to extract approximately 86% of the zinc present in the CW sample.

The extraction value obtained is comparable to that found by Clay and Schoonraad (1976), who treated a blend of willemite concentrate and tailings using the Waelz process. They obtained a zinc extraction of approximately 90% at 1100°C using a 30% addition of reducing material (anthracite duff, coke breeze, and reclaimed reductant). According to Harris (1936), some industrial plants were able to treat calamine waste by adding only 10–12% coke to the Waelz furnace, although the coke addition used in industrial processes typically ranges from 20–35%. It is noteworthy that values as high as 45–55% coke in feed material were reported in zinc production.

After determining the optimum amount of CV needed to reduce willemite concentrate, experiments were carried out to determine the influence of temperature on zinc extraction (Figure 12). The results show that zinc extraction decreases with decreasing temperature, the highest extraction of 86% being obtained at 1100°C. Other authors who utilized different zinc-bearing materials have also reported this temperature as the optimal. Furthermore, the formation of accretions has been observed at temperatures exceeding 1200°C (Clay and Schoonraad, 1976). Industrial processes typically operate at temperatures close to 1100°C. (Krupka, Ochab, and Miernik, 2000; Harris, 1936).

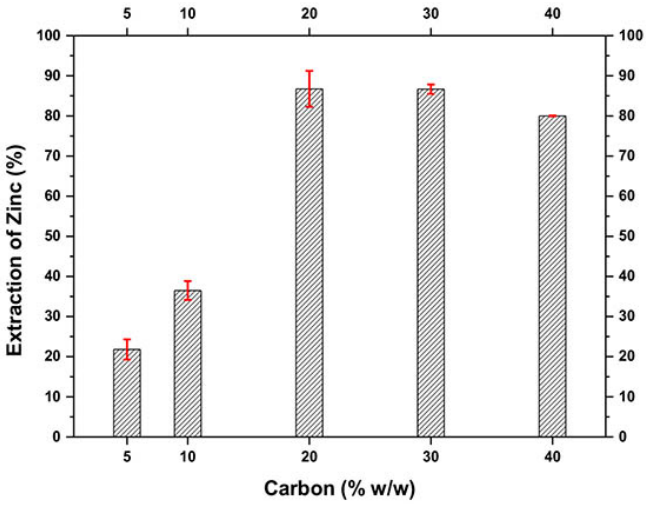

Figure 11—Influence of charcoal addition on zinc extraction from the CW sample by carbothermic reduction (T =1100°C; time = 1 h)

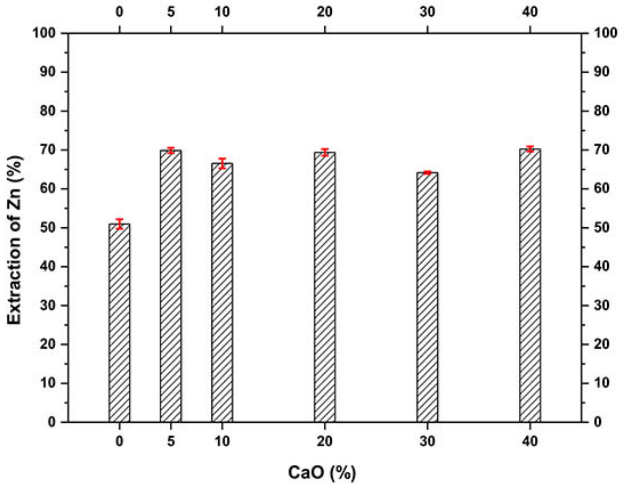

Figure 12—Influence of temperature on zinc extraction from CW sample by carbothermic reduction (20% C; time = 1 h)

As shown in the TGA curves (Figure 10), the presence of CaO in the concentrate promoted an increase in mass loss. Thus, reduction tests were performed in a tubular furnace aiming to evaluate the influence of CaO on zinc extraction (Figure 13). The results show that the presence of CaO significantly increased zinc extraction during carbothermic reduction at 1050°C. A CaO addition of only 5% increased zinc extraction by 34%. As discussed earlier, this increase can be ascribed to the promotion of the thermal decomposition of willemite by CaO (Equations [13] and]14]).

The effect of temperature on zinc extraction in reduction tests with CaO is shown in Figure 14. The addition of CaO improved zinc extraction at all temperatures (Figure 15). The best extraction (93%) was obtained at a temperature of 1100°C for 1 hour with 5% CaO addition and 20% carbon.

The basicity of the slag generated by the Waelz process is determined by Equation [19]:

$$\text{Basicity } (B) = \frac{(\%CaO+\%MgO)}{\%SiO_2} \quad [19]$$

where %MO is the percentage of metallic oxide in the slag. Basicities between 0.2 and 0.5 denote an acid process, and values from 1.5 to 4 a basic process. The operational control of a Waelz plant between these two conditions is exceptionally challenging (Mager *et al.*, 2000; Mattich *et al.*, 1998).

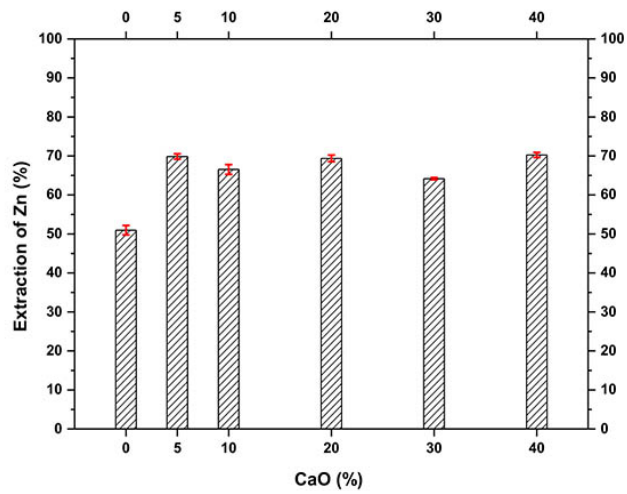

Figure 13— Influence of the amount of CaO addition on the extraction of zinc from the CW sample by carbothermic reduction (time = 1 h; 1050°C; 20% CV)

Assuming that the major mineral constituents of the sample (willemite and dolomite) were effectively reduced (Equation [9]) and calcined (Equation [7]), the estimated basicity (B) of the process, based on the experiments performed with varying quantities of CaO, ranges from 0.32 (0 % CaO) to 1.75 (40% CaO). This suggests that, besides enhancing the extraction of Zn, the addition of CaO will also contribute to better process control. Analysis of the slag generated at 1100°C, reaction time 1 hour, with with 5% CaO and 20% carbon yielded a calculated basicity of 0.38.

Conclusion

It was possible to obtain approximately 86% zinc extraction from a willemite concentrate using charcoal as a reducing agent at a temperature of 1100°C for 1 hour reaction time. The extraction values increased with increasing temperature, and the best results were obtained with 20% charcoal in the charge. During the reduction, the calcination of dolomite, present as a gangue constituentin the concentrate, promoted the formation of calcium oxide, which reacted with willemite to form zinc oxide and calcium silicates. The formation of zinc oxide allowed reduction of the concentrate to begin at a temperature 60°C lower than the minimum thermodynamic temperature for the reduction of willemite.

The addition of only 5% CaO to the willemite concentrate improved the zinc extraction at all temperatures studied. At a temperature of 1100°C, with 20% C and 5% CaO, it was possible to extract approximately 93% Zn, 8% more than without addition of CaO under the same conditions.

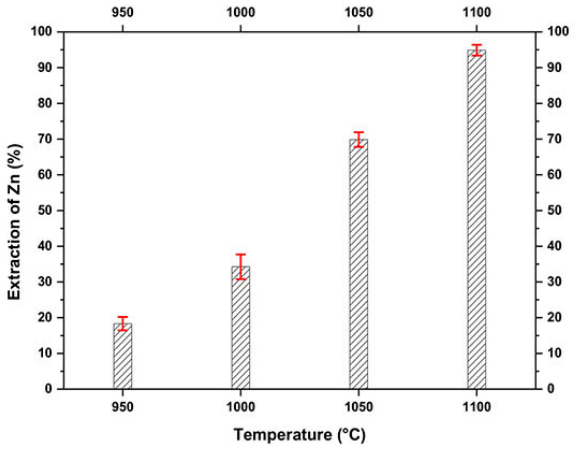

Figure 14—Influence of temperature on zinc extraction from willemite concentrate in the presence of CaO (time = 1 h; 5% CaO; 20% CV)

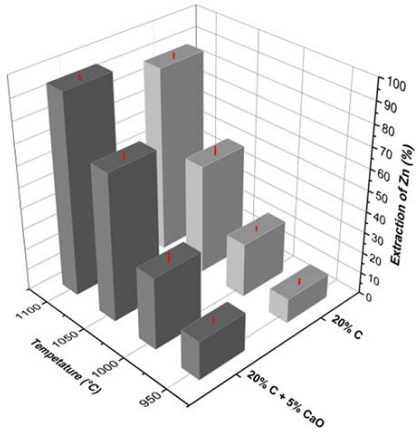

Figure 15—Zinc extraction from the CW sample in the presence and absence of CaO

Acknowledgement

This study was financed in part by the Fundação de Amparo à Pesquisa do Estado de Minas Gerais — Brazil (Fapemig) and the Coordenação de Aperfeiçoamento de Pessoal de Nível Superior (CAPES) [Coordenação de Aperfeiçoamento de Pessoal de Nível Superior]. The authors are also grateful to the Conselho Nacional de Desenvolvimento Científico e Tecnológico (CNPq) for the partnership and financial support throughout the research.

Credit author statement

VSC – Writing; Methodology; Investigation.
GML – Writing; Funding acquisition; Reviewing.
VAL – Validation; Resources; Funding acquisition.
RFMS – Validation; Funding acquisition; Reviewing and Edition.
VAO – Conceptualization; Methodology; Investigation; Supervision; Validation; Resources; Writing; Visualization; Funding acquisition.

Conflict of interest

On behalf of all authors, the corresponding author states that the authors have no known competing financial interests or personal relationships that could have appeared to influence the work reported in this paper.

References

Antuñano, N., Herrero, D., Arias, P.L., and Cambra, J.F. 2013, Electrowinning studies for metallic zinc production from double leached Waelz oxide. *Process Safety and Environmental Protection*, vol. 91. pp. 495–502. https://doi.org/10.1016/j.psep.2012.10.014

Antuñano, N., Arias, P.L., and Cambra, J.F. 2019. Hydrometallurgical processes for Waelz oxide valorisation – An overview. *Process Safety and Environmental Protection*, vol. 129. pp. 308–320. https://doi.org/10.1016/j.psep.2019.06.028

Boni, M. and Mondillo, N. 2015. The 'Calamines' and the 'Others': The great family of supergene non-sulfide zinc ores. *Ore Geology Reviews*, vol. 67. pp. 208–233. https://doi.org/10.1016/j.oregeorev.2014.10.025

Chen, H.K. 2001. Kinetic study on the carbothermic reduction of zinc oxide. *Scandinavian Journal of Metallurgy*, vol. 30. pp. 292–296. https://doi.org/10.1034/j.1600-0692.2001.300503.x

Clay, J.E.G. and Schoonraad, P. 1976. Treatment of zinc silicates by Waelz Process. *Journal of the South African Institute of Mining and Metallurgy*, vol. 77. pp. 11–14.

Dill, H.G. 2010. The 'chessboard' classification scheme of mineral deposits: Mineralogy and geology from aluminium to zirconium. *Earth Science Reviews*, vol. 100. pp. 148–174. https://doi.org/10.1016/j.earscirev.2009.10.011

Harris, W.E. 1936. The Waelz Process. AIME Transactions, vol. 121. *Metallurgy of Lead and Zin*. pp. 702–720.

Herce, C., Stendardo, S., and Cristóbal, C. 2015. Increasing CO2 carrying capacity of dolomite using thermal stabilization by triggered calcination. *Chemical Engineering Journal*, vol. 262. pp. 18–28. https://doi.org/10.1016/j.cej.2014.09.076

James, S.E. and Bound, C.O. 1990. Recycling lead and cadmium, as well as zinc, from EAF dust. Lead-Zinc ´90: *Proceedings of a World Symposium on Metallurgy and Environmental Control*. Mackey, T.S. and Pregaman, R.D. (eds). The Minerals, Metals & Materials Society, Anaheim CA. pp. 477–495.

Krupka, D., Ochab, B., and Miernik, J. 2000. The Boleslaw electrolytic zinc plant. *Proceedings of Lead-Zinc 2000*. Dutrizac, J.E., Gonzalez, J.A., Henke, D.M., James, S.E., and Siegmund, A.H.J. (eds). The Minerals, Metals & Materials Society, Warrendale, PA. pp. 277–286.

Li, Q.X., Hu, H.P., Zeng, D.W., and Chen, Q.Y. 2013. Solubility of hemimorphite in ammonium sulfate solution at 25°C. *Transactions of Nonferrous Metals Society of China*, vol. 23. pp. 2160–2165. https://doi.org/10.1016/S1003-6326(13)62712-0

Liu, Z., Liu, Z., Li, Q., Cao, Z., and Yang, T. 2012. Dissolution behaviour of willemite in the $(NH_4)_2SO_4$–NH_3–H_2O system. *Hydrometallurgy*, vol. 125–126. pp. 50–54. https://doi.org/10.1016/j.hydromet.2012.05.006

Mager, K., Meurer, U., Garcia-Egocheaga, B., Goicoechea, N., Rutten, J., Saage, W., and Simonetti, W.F. 2000. Recovery of zinc oxide from secondary raw materials: New development of the Waelz process. *Fourth International Symposium on Recycling of Metals and Engineered Materials. Proceedings of the TMS Fall Extraction and Processing Conference*. Stewart, D.L., Stephens R., and Daley, J.C. (eds). The Minerals, Metals & Materials Society, Warrendale, PA. pp. 329–344. https://doi.org/10.1002/9781118788073.ch29

Mattich, C., Hasselwander, Lommert, K., and Beyzavi, H.A.N. 1998, Electrolytic zinc manufacture with Waelz treatment of neutral leach residues. *Proceedings of Lead and Zinc Processing*. JCIM, Montreal. pp. 561–578.

Oliveira, V.A.A., Penna, J.M.S., Magalhães, L.S., Leão, V.A., and dos Santos, C.G. 2019, Kinetics of copper and cádmium cementation by zinc powder. *Tecnologia em Metalurgia, Materiais e Mineração*, vol. 16. pp. 255–262. http://dx.doi.org/10.4322/2176-1523.20191661

Ptáček, P., Šoukal, F., and Opravil, T. 2021. Thermal decomposition of ferroan dolomite: A comparative study in nitrogen, carbon dioxide, air and oxygen. *Solid State Sciences*, vol. 122. pp. 106778. https://doi.org/10.1016/j.solidstatesciences.2021.106778

Safari, V., Arzpeyma, G., Rashchi, F., and Mostoufi, N. 2009, A shrinking particle—shrinking core model for leaching of a zinc ore containing silica. *International Journal of Mineral Processing*, vol. 93. pp. 79–83. https://doi.org/10.1016/j.minpro.2009.06.003

Santos, F.M.F., Pina, P.S., Porcaro, R., Oliveira, V.A.A., Silva, C.A., and Leão, V.A. 2010. The kinetics of zinc silicate leaching in sodium hydroxide, *Hydrometallurgy*, vol. 102. pp. 43–49. https://doi.org/10.1016/j.hydromet.2010.01.010

Sinclair, R.J. 2005. The Extractive Metallurgy of Zinc. 1st edn. *Spectrum Series*, vol. 13. Australasian Institute of Mining and Metallurgy, Melbourne.

Souza, A.D., Pina, P.S., Leão, V.A., Silva, C.A.m and Siqueira, P.F. 2007a. The leaching kinetics of a zinc sulfide concentrate in acid ferric sulphate, *Hydrometallurgy*, vol 89 pp. 72–81. https://doi.org/10.1016/j.hydromet.2007.05.008

Souza, A.D., Pina, P.S., Lima, E.V.O., da Silva, C.A., and Leão, V.A. 2007b. Kinetics of sulfuric acid leaching of a zinc silicate calcine. *Hydrometallurgy*, vol. 89. pp. 337–345. https://doi.org/10.1016/j.hydromet.2007.08.005

Wahab, R., Ansari, S.G., Kim, Y.S., Dar, M.A., and Shin, H.S. 2008. Synthesis and characterization of hydrozincite and its conversion into zinc oxide nanoparticles. *Journal of Alloys and Compounds*, vol. 461. pp. 66–71. https://doi.org/10.1016/j.jallcom.2007.07.029

Wang, J., Zhang, Y., Cui, K., Fu, T., Gao, J., Hussain, S., and AlGarni, T.S. 2021. Pyrometallurgical recovery of zinc and valuable metals from electric arc furnace dust – A review. *Journal of Cleaner Production*, vol. 298. pp. 126788. https://doi.org/10.1016/j.jclepro.2021.126788

Xiong, L.Z., Chen, Q.Y., Yin, Z.L. Zhang, P.M., Ding, Z.Y., and Liu, Z.X. 2012. Preparation of metal zinc from hemimorphite by vacuum carbothermic reduction with CaF2 as catalyst. *Transactions of Nonferrous Metals Society of China*, vol. 22. pp. 694–699. https://doi.org/10.1016/S1003-6326(11)61233-8

Xiong, L.Z., Xiang, Y.H., Wu, X.W., He, Z.Q., and Yin, Z.L. 2017. Preparation of high purity zinc from zinc oxide ore by vacuum carbothermic reduction. *Vacuum*, vol. 146. pp. 200–205. https://doi.org/10.1016/j.vacuum.2017.09.050

Yin, Z., Ding, Z., Hu, H., Liu, K., and Chen, Q. 2010, Dissolution of zinc silicate (hemimorphite) with ammonia–ammonium chloride solution. *Hydrometallurgy*, vol. 103, no. 1–4. pp. 215-220. https://doi.org/10.1016/j.hydromet.2010.03.006

Zhang, Q., Wen, S., Wu, D., Feng, Q., and Li, S. 2019. Dissolution kinetics of hemimorphite in trichloroacetic acid solutions. *Journal of Materials Research and Technology*, vol. 8. pp. 1645–1652. https://doi.org/10.1016/j.jmrt.2018.11.010

Zhang, X., Chen, L., Sun, Y., Bai, Y., Huang, B., and Chen, K. 2018. Determination of zinc oxide content of mineral medicine calamine using near-infrared spectroscopy based on MIV and BP-ANN algorithm. *Spectrochimica Acta Part A: Molecular and Biomolecular Spectroscopy*, vol. 193. pp. 133–140. https://doi.org/10.1016/j.saa.2017.12.019

Zhang, Y., Deng, J., Chen, J., Yu, R., and Xing, X. 2014. A low-cost and large-scale synthesis of nano-zinc oxide from smithsonite. *Inorganic Chemistry Communications*, vol. 43. pp. 138–141. https://doi.org/10.1016/j.inoche.2014.02.032

Zhao, D., Yang, S., Chen, Y., Tang, C., He, J., and Li, H. 2017. Leaching kinetics of hemimorphite in ammonium chloride solution. *Metals*, vol. 7. pp. 237. https://doi.org/10.3390/met7070237 ◆